

Relativistic heavy ion collisions with realistic non-equilibrium mean fields

C. Fuchs^a T. Gaitanos^b H. H. Wolter^b

^a*Institut für Theoretische Physik der Universität Tübingen, D-72076 Tübingen, Germany*

^b*Sektion Physik, Universität München, D-85748 Garching, Germany*

Abstract

We study the influence of non-equilibrium phase space effects on the dynamics of heavy ion reactions within the relativistic BUU approach. We use realistic Dirac-Brueckner-Hartree-Fock (DBHF) mean fields determined for two-Fermi-ellipsoid configurations, i.e. for colliding nuclear matter, in a local phase space configuration approximation (LCA). We compare to DBHF mean fields in the local density approximation (LDA) and to the non-linear Walecka model. The results are further compared to flow data of the reaction Au on Au at 400 MeV per nucleon measured by the FOPI collaboration. We find that the DBHF fields reproduce the experiment if the configuration dependence is taken into account. This has also implications on the determination of the equation of state from heavy ion collisions.

Key words: Relativistic BUU, non-equilibrium mean fields, local configuration approximation, Dirac-Brueckner-Hartree-Fock, $Au+Au$, $E=400$ MeV/nucleon reaction, transverse flow, equation of state.

PACS numbers: **21.65.+f**, **25.75.+r**

1 Introduction

A principal object of the investigation of heavy ion collisions at intermediate energies is to determine the nuclear equation of state (EOS), i.e. the properties of nuclear matter in equilibrium away from saturation and at non-zero temperatures. However, the phase space distribution in a heavy ion collision is out of global and even local equilibrium through most of the collision time. Thus transport models have been developed to describe the evolution of the phase space [1–5]. Although these models are quite successful to reproduce data the attempts to determine the EOS, e.g., from the transverse flow in heavy ion collisions have not led to generally accepted results. Recently also

experimental collaborations, like FOPI or EOS, again focused on this problem [6,7].

The difficulty is in part due to the non-equilibrium effects mentioned above. The common practice of theoretical calculations is to apply phenomenological mean fields like Skyrme forces [2] in a non-relativistic or the Walecka model [8] and its non-linear extensions in a relativistic approach [4,9]. These forces contain parameters which allow to vary the characteristics of the corresponding EOS. In some cases a phenomenological momentum dependence taken from the empirical nucleon-nucleus optical potential has been added [2,10]. However, non-equilibrium features of the phase space are not contained in these forces, a fact which certainly will lead to uncertainties when conclusions on the ground state EOS are drawn.

A derivation of a kinetic equation from a microscopic non-equilibrium many-body theory shows that a consistent treatment requires to determine the effective interaction in the nuclear medium for the non-equilibrium phase space configurations of heavy ion collisions [11]. Generally, the Dirac-Brueckner-Hartree-Fock (DBHF) theory provides a very successful approach to the many-body problem in nuclear matter [12,13] and in finite nuclei [14–16]. However, a solution of the Bethe-Salpeter equation for arbitrary anisotropic momentum configurations is extremely difficult. Approximate treatments should retain the most important features of such configurations. To improve on the local density approximation (LDA) the phase space has been represented locally by two Fermi ellipsoids separated by a relative momentum. We have called this the *local configuration approximation* (LCA) [17]. In contrast to the LDA which refers to ground state nuclear matter the LCA describes colliding nuclear matter (CNM) and should be able to reproduce the main features of the anisotropic momentum space in a heavy ion collision over the entire reaction time.

However, even for the idealized momentum configuration of two Fermi ellipsoids the Bethe-Salpeter equation has not yet been solved. Only in a non-relativistic framework this problem has been treated before [18]. Therefore as a first step Sehn et al. [19,20] developed a procedure to construct self-energies for colliding nuclear matter from an appropriate parametrization of DBHF ground state results. These self-energies take into account specific non-equilibrium features of the momentum space and approximately include the correlations of the T -matrix. Rather than introducing model parameters as, e.g. in the Skyrme or the Walecka model, the DBHF mean fields are connected in a parameterfree way to the free NN-interaction. In this sense we call these fields "realistic".

We compare the present approach to experiment, i.e. to FOPI flow data of the system Au on Au at 400 A.MeV [6,21]. In addition we compare to the

LDA and to a standard force used in relativistic heavy ion calculations, the non-linear Walecka model (NL2).

2 DBHF Mean Fields in the RBUU Approach

As shown, e.g., in Ref. [11] the self-energy $\Sigma = \Sigma_s - \gamma^\mu \Sigma_\mu$ which enters into the relativistic Boltzmann-Uehling-Uhlenbeck (RBUU) equation

$$\left[p^{*\mu} \partial_\mu^x + (p_\nu^* F^{\mu\nu} + m^* \partial_x^\mu m^*) \partial_\mu^{p^*} \right] f(x, p^*) = I_C \quad (1)$$

via effective masses $m^* = M + \text{Re}\Sigma_s$, kinetic momenta $p_\mu^* = p_\mu + \text{Re}\Sigma_\mu$, and the field strength tensor $F^{\mu\nu}$ in principle has to be determined from the corresponding T -matrix in non-equilibrium. Consistently with the kinetic equation (1) we represent Σ in Hartree form by separating off a linear density dependence through the definition of dynamical coupling functions

$$\text{Re}\Sigma[f] = -\Gamma_s[f] \rho_s[f] + \gamma_\mu \Gamma_0[f] j^\mu[f] \quad . \quad (2)$$

In Eq. (2) ρ_s and j^μ are the scalar density and the baryonic four-current, respectively, and $[f]$ denotes the dependence on the phase space distribution f . The self-energy, Eq. (2), is of the same structure as the mean field in the $\sigma\omega$ -model [8], however, the coupling constants $\frac{g_\sigma^2}{m_\sigma^2}$, $\frac{g_\omega^2}{m_\omega^2}$ for the scalar (σ) and the vector (ω) meson are replaced by the dynamical coupling functions $\Gamma_{s,0}[f]$. These are Lorentz scalars and given by invariants of the T -matrix averaged over f [20]. In the LCA the $\Gamma_{s,0}$, Eq. (2), are locally approximated by the values for the corresponding colliding nuclear matter configurations, and thus depend on the collective parameters of the CNM configuration, i.e. the Fermi momenta and the relative velocity of the local currents

$$\Gamma_{s,0}[f] \longmapsto \bar{\Gamma}_{s,0}^{(12)}(p_{F_1}, p_{F_2}, v_{\text{rel}}) \quad . \quad (3)$$

In this formulation the LDA means to use $\bar{\Gamma}(p_{F_{\text{tot}}})$ corresponding to a single Fermi sphere at the respective total density. The calculation of the $\bar{\Gamma}_{s,0}^{(12)}$ is discussed in detail in Ref. [20]. They are constructed by extrapolating the density and momentum dependent coupling functions $\Gamma_{s,0}(p, \rho_B)$ defined as in Eq. (2) for DBHF nuclear matter calculations to CNM configurations. There we used the DBHF results of Ref. [13] (without Δ -particles). Thus the $T=0$ EOS is the one given in Fig. 3.8 of Ref. [13], which gives a good fit of the saturation properties, an incompressibility of 250 MeV, and a good reproduction of the energy dependence of real part of the optical potential up to about 400 MeV.

In the LCA the collective parameters of the CNM configurations are determined in every time step from the actual phase space distribution. To do so f is decomposed into the respective contributions from projectile and target $f = f^{(1)} + f^{(2)}$. The Fermi momenta $p_{F_i} = (2/3\pi^2\rho_0^{(i)})^{\frac{1}{3}}$ are defined in the rest frames of the currents by an invariant rest density [17,19]

$$\rho_0^{(i)}(x) = \sqrt{j_\mu^{(i)}(x)j^{(i)\mu}(x)} \quad , \quad i = 1, 2 \quad (4)$$

$$j_\mu^{(i)}(x) = 4 \int \frac{d^3p}{(2\pi)^3} \frac{p_\mu^*}{E^*} f^{(i)}(x, \vec{p}) = u_\mu^{(i)}(x) \rho_0^{(i)}(x) \quad . \quad (5)$$

The invariant relative velocity $v_{\text{rel}} = |\vec{v}_{\text{rel}}|$ is obtained from the streaming velocities $u_\mu^{(i)} = (u_0^{(i)}, \vec{u}^{(i)})$ as

$$\vec{v}_{\text{rel}}(x) = \frac{u_0^{(2)}\vec{u}^{(1)} - u_0^{(1)}\vec{u}^{(2)}}{u_\mu^{(1)}u^{(2)\mu}} \quad . \quad (6)$$

In the present calculations we assume symmetric configurations, i.e. $p_{F_1} = p_{F_2}$, which is a good approximation to the participant region. For highly asymmetric configurations where one density falls significantly below the other, what mainly occurs in the more peripheral reactions, the system is treated as one Fermi sphere in the LDA.

To give an impression of the configuration effects we show in Fig. 1 the Schrödinger equivalent real part of the optical potential as a function of E_{lab} . The DBHF nucleon optical potential in a nucleus–nucleus collision in the CNM approximation [20] is compared to the corresponding nucleon–nucleus optical potential [13] at the same density. In CNM the energy dependence of U_{opt} originates from the dependence of the mean field on $v_{\text{rel}}(E_{\text{lab}})$ whereas in the LDA, also shown in Fig. 1, the self-energy is taken at the corresponding density and kept constant. In the latter case $\text{Re}U_{\text{opt}}$ scales linearly with energy as is the case, e.g., also in the Walecka model [4,8]. The configuration dependence (LCA) significantly softens the optical potential leading to a similar behavior as in nuclear matter when the full momentum dependence of the self-energy is included [13]. At two times saturation density the nucleus–nucleus optical potential is even softer. More exactly speaking we use "cold" CNM configurations to parametrize the phase space distribution, i.e. two sharp Fermi spheres. More consistently one could use two Fermi spheres of finite temperature. In a forthcoming work we analysed the phase space distribution in such a way and we find temperatures of less than about 30 MeV. In Ref. [13] it is found that $\text{Re}U_{\text{opt}}$ is only weakly changed at these temperatures and thus the assumption of zero temperature fields appears justified.

For the solution of the relativistic BUU equation we use the relativistic Landau-Vlasov method [5] which represents the phase space distribution by covariant gaussian testparticles in coordinate and momentum space. A fully consistent treatment of the kinetic equation in principle requires to treat the in-medium cross section on the same footing as the mean field [11]. Hence in Ref. [22] an in-medium cross section has been derived for CNM from the imaginary part of the DBHF self-energies. However, in this work we focus on the mean field and apply the standard Cugnon parametrization [23] for the cross section. As shown, e.g., in Ref. [25] the transverse flow does not react very sensitively to the cross section and we do not expect the present results to be significantly altered by the use of a consistently determined in-medium cross section.

3 The System Au on Au at 400 A.MeV

The present system is particularly well adapted to study non-equilibrium effects. The bombarding energy is high enough to result in distinct two-Fermi-ellipsoid momentum configurations in the initial phase of the reaction and the

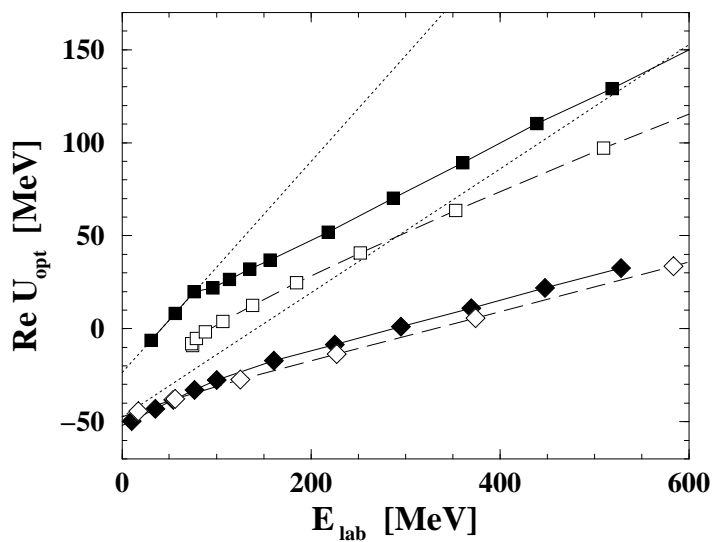


Fig. 1. Energy dependence of the DBHF optical potential. The solid lines represent the nucleon–nucleus optical potential taken from ref. [13] at saturation density ρ_{sat} (diamonds) and $2\rho_{\text{sat}}$ (squares). The dashed lines represent the corresponding nucleon optical potential in a nucleus–nucleus collision determined in the colliding nuclear matter approximation at subsystem densities $\rho_0^{(1)} + \rho_0^{(2)} = \rho_{\text{sat}}$ (diamonds) and $\rho_0^{(1)} + \rho_0^{(2)} = 2\rho_{\text{sat}}$ (squares). The dotted lines refer to the DBHF nucleon–nucleus optical potential obtained in a simple LDA with no momentum dependence included at densities ρ_{sat} (lower curve) and $2\rho_{\text{sat}}$ (upper curve).

densities reached in the compression phase are sufficiently high to test the density dependence of the EOS. Impact parameter selected high quality data of nuclear flow are provided by the FOPI collaboration [6]. Fig. 2 shows the

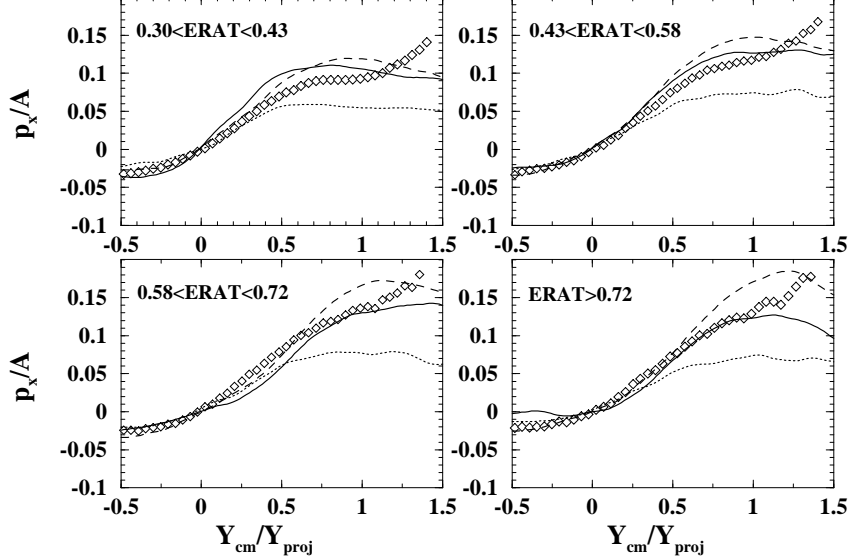


Fig. 2. Transverse flow per nucleon in units of the nucleon mass for the reaction Au on Au at 400 A.MeV. Four $ERAT$ bins running from semi-peripheral (top left) to central collisions (bottom right) collisions have been selected. Non-equilibrium DBHF mean fields were used (solid curves) as well as DBHF mean fields in the LDA (dashed curves). The dotted curves correspond to the non-linear Walecka model NL2 and the diamonds represent the FOPI data of Ref. [6].

in-plane transverse flow per particle p_x/A in units of the nucleon mass for four different $ERAT$ bins. $ERAT$ is defined as the ratio of transversal to longitudinal kinetic energy deposited in the forward center-of-mass hemisphere [6] and provides a measure for the impact parameter bins which run from semi-peripheral ($b \simeq 6$ fm, $0.30 \leq ERAT \leq 0.43$) to central ($ERAT \geq 0.72$) collisions. For the analysis of the reaction we use the geometrical part of the FOPI filter [24] which takes into account acceptance cuts for different mass fragments. We therefore generated fragments after the collision (60 fm/c) by a phase space coalescence model. The influence of the filter on the observables is similar as in Ref. [6]. For the original experimental data the crossover of the flow from negative to positive values is slightly shifted to positive center-of-mass rapidity values. This behavior is quantitatively not well understood but is supposed to be due to recoil effects or double hits [24]. After applying the filter analysis the crossover of the theoretical curves is slightly shifted to negative rapidities. For a better comparison of the flow, i.e. the slope of p_x/A , in Fig. 2 we readjusted the crossovers to $p_x/A = 0$ for theory and experiment.

It is seen from Fig. 2 that the non-equilibrium DBHF mean fields (LCA) are

able to reasonably reproduce the data. The configuration dependence of the fields weakens their repulsion, as seen in Fig.1, resulting in less flow compared to a pure LDA treatment. This configuration effect on the flow is strongly increasing with centrality and reaches a magnitude comparable to different equations of state, i.e. about 30% of the total amount of flow. This can be understood by the increasing overlap of the nuclei since only the participant matter feels configuration effects. For the spectator matter our description always results in a LDA treatment. We also find that over the entire impact parameter range NL2 yields a too small transverse flow compared to the experiment.

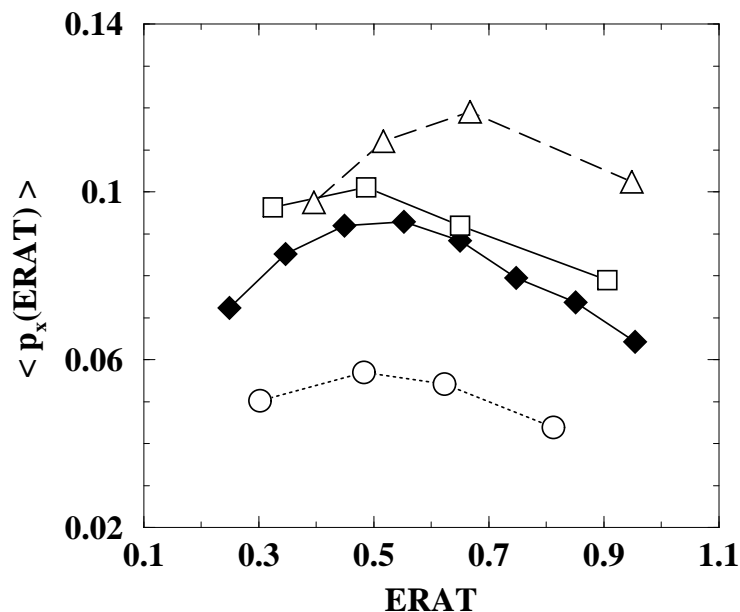


Fig. 3. Total transverse flow averaged over the forward cms hemisphere in units of the nucleon mass for the same reaction as in Fig.2. Non-equilibrium DBHF mean fields were used (squares) as well as DBHF mean fields in the LDA (triangles). The circles correspond to the non-linear Walecka model NL2 and the diamonds represent the FOPI data of Ref. [6].

In Fig.3 we show the total amount of flow $\langle p_x(ERAT) \rangle$ integrated over the forward center-of-mass hemisphere. Again, the LCA calculations are close to the data and also reproduce best the shape over the entire $ERAT$ range. The larger deviation in the more peripheral collisions is probably due to the fact that the CNM mean fields are always determined for symmetric configurations ($p_{F_1} = p_{F_2}$). For the very central collisions (high $ERAT$ values) the LDA completely fails and overestimates the data by about a factor of 2 but becomes more reliable with increasing impact parameter. The NL2 model again strongly underestimates the flow.

Table 1

Mean directed in-plane transverse flow normalized to the center-of-mass projectile momentum per nucleon. Calculations were performed with DBHF mean fields in non-equilibrium (LCA) as well as in the local density approximation (LDA) and with the non-linear Walecka model NL2. The experimental value is taken from Ref. [21].

	DBHF		NL2	EXP
	LCA	LDA		
$P_x^{\text{dir}}/P_{CM}^{\text{proj}}$	0.187	0.232	0.103	0.173

The above results are summarized in Table 1. There the mean in-plane directed transverse flow normalized to the center-of-mass projectile momentum per nucleon is given. The experimental value [21] has been obtained for the PM4 event class corresponding to semi-central ($3 \leq b \leq 5$) collisions. This quantity provides a good measure of the global repulsion of the model. The DBHF result is close to the experimental value when treated in the local configuration approximation (LCA). The local density approximation (LDA) overestimates the experiment by about 30% and the NL2 parameter set of the non-linear Walecka model underestimates the data by about 40%.

To understand the influence of the mean field on the reaction dynamics we emphasize that in a relativistic approach the major part of the repulsion is due to Lorentz forces generated by the vector field (see Fig. 1). The repulsion and, correspondingly, the stiffness of the EOS in first order is given by the effective mass; the smaller the effective mass the more repulsive is the model [3,10]. Thus NL2 with a large effective mass ($m^*/m_0=0.83$) is relatively soft whereas the DBHF EOS ($m^*/m_0=0.586$) is rather stiff. The momentum dependence of the mean field which is taken into account in the LCA in an averaged form actually weakens this repulsion as also found in Ref. [10]. The small vector fields of NL2 lead to an underestimation of the flow. Furthermore, the density dependence of NL2 is too small to produce a sufficient amount of flow just by compression. Thus the use of parametrizations with a stiffer EOS but with the same m^* will not significantly improve on this [4].

The same reaction as above has been analyzed in the QMD approach in Ref. [6] using forces based on the non-relativistic ground state BHF G -matrix [18,25]. There it was found that the strong and repulsive momentum dependence of the G -matrix is necessary to reproduce the data of the more peripheral collisions. However, in the more central collisions the non-relativistic G -matrix lacks a sufficient density dependence and results in a too small flow [6]. This drawback is resolved in a relativistic approach where the T -matrix provides the appropriate balance between density and momentum dependence.

4 Summary and Conclusions

Realistic DBHF mean fields have been used in a detailed flow analysis of heavy ion collisions at intermediate energies. We have taken into account non-equilibrium features of the phase space in a local configuration approximation using mean fields determined for a colliding nuclear matter scenario. The ground state DBHF self-energies are rather repulsive relative to, e.g., standard parametrizations of the non-linear Walecka model. However, if the configuration effects are taken into account properly the DBHF mean fields are able to reproduce the overall behavior of the experimental flow data. Thus, the configuration effects turned out to be of major importance, especially if more central collisions are considered. A simple LDA treatment results in too repulsive mean fields. The intrinsic momentum dependence of the local configuration approximation weakens this repulsion considerably. An extension of the colliding nuclear matter approximation to anisotropic configurations and the inclusion of finite temperature effects and of an in-medium cross section may still improve the present results. A more detailed comparison to data including also longitudinal flow variables will be forthcoming.

To summarize we conclude that DBHF mean fields based on realistic NN interactions are able to reproduce intermediate energy flow data, thus testing the DBHF approach also at high densities. It is found that the inclusion of non-equilibrium effects is important in order to learn something about the equation of state of ground state nuclear matter.

Acknowledgements

The authors would like to thank L. Sehn for valuable discussions. In particular, we thank W. Reisdorf and P. Dupieux for helpful discussions with respect to the comparison to the data and for providing us with the FOPI filter simulation code.

References

- [1] G.F. Bertsch and S. Das Gupta, Physics Reports **160** (1988) 190.
- [2] J. Aichelin, H. Stöcker, Phys. Lett. **B176** (1986) 14.
- [3] Q. Li, J.Q. Wu, C.M. Ko, Phys. Rev. **C39** (1989) 849.
- [4] B. Blättel, V. Koch, U. Mosel, Rep. Prog. Phys. **56** (1993) 1.

- [5] C. Fuchs, H.H. Wolter, Nucl. Phys. **A589** (1995) 732.
- [6] The FOPI Collaboration, Nucl. Phys. **A587** (1995) 802.
- [7] The EOS collaboration, Phys. Rev. Lett. **75** (1995) 2100.
- [8] J.D. Walecka, Ann. Phys. (N.Y.) **83** (1974) 497.
- [9] J. Boguta, A.R. Bodmer, Nucl. Phys. **A292** (1977) 413.
- [10] T. Maruyama, W. Cassing, U. Mosel, S. Teis and K. Weber, Nucl. Phys. **A573** (1994) 653.
- [11] W. Botermans, R. Malfliet, Phys. Rep. **198** (1990) 115.
- [12] C.J. Horowitz, B.D. Serot, Nucl. Phys. **A464** (1987) 613.
- [13] B. ter Haar, R. Malfliet, Phys. Rep. **149** (1987) 207.
- [14] R. Brockmann, H. Toki, Phys. Rev. Lett. **68** (1992) 3408.
- [15] H.F. Boersma and R. Malfliet, Phys. Rev. **C49** (1994) 233.
- [16] C. Fuchs, H. Lenske, H.H. Wolter, Phys. Rev. **C52**, (1995) 3043.
- [17] C. Fuchs, L. Sehn, H.H. Wolter, Nucl. Phys. **A545** (1992) 151c.
- [18] J. Jaenicke, J. Aichelin, N. Ohtsuka, R. Linden, A. Faessler, Nucl. Phys. **A536** (1992) 201.
- [19] L. Sehn, H.H. Wolter, Nucl. Phys. **A519** (1990) 289c.
- [20] L. Sehn, H.H. Wolter, Nucl. Phys. **A** in press.
- [21] A. Gobbi for the FOPI colaboration, Nucl. Phys. **A583** (1996) 499.
- [22] C. Fuchs, L. Sehn, H.H. Wolter, Nucl. Phys. **A** in press.
- [23] J. Cugnon, T. Mizuani and J. Vandermeulen, Nucl. Phys. **A352** (1981) 505.
- [24] W. Reisdorf, P. Dupieux, private communication.
- [25] D.T. Khoa, N. Ohtsuka, M.A. Martin, A. Faessler, S.W. Huang, E. Lehmann and R.K. Puri, Nucl. Phys. **A548** (1992) 102.